Time and Frequency Domain Analysis of Memristor Based Series and Parallel RLCM Circuits

T. D. Dongale[1], A. R. Chavan[1], S. S. Sutar[2], A. M. Mane[2], Ch. K. Volos[3], P. K. Gaikwad[4], R. K. Kamat[4]
[1]*Computational Electronics and Nanoscience Research Laboratory, School of Nanoscience and Biotechnology, Shivaji University, Kolhapur 416004, India.*
[2]*Yashwantrao Chavan School of Rural Development, Shivaji University, Kolhapur 416004, India.*
[3]*Physics Department, Aristotle University of Thessaloniki, Thessaloniki 54124, Greece.*
[4]*Department of Electronics, Shivaji University, Kolhapur, 416004, India.*
tdd.snst@unishivaji.ac.in

***Abstract*—The paper investigates the state space analysis of memristor based series and parallel RLCM circuits. The stability analysis was carried out with the help of eigenvalues formulation method, pole-zero plot and transient response of system. The state space analysis was successfully applied and eigenvalues of the two circuits were calculated. It was found that the system followed a negative real part of eigenvalues. The result clearly shows that addition of memristor in circuits does not alter the stability of the system. It was found that systems' poles are located at left hand side of the S plane, which indicates a stable performance of system. It is clear that the eigenvalues have negative real part; hence the two systems are internally stable. Furthermore, the time and frequency domain resulting from both the systems suggest the stability of bounded input and bounded output (BIBO).**

***Index Terms*—Memristor; State Space Analysis; Pole-Zero Plots; Stability.**

I. INTRODUCTION

Memristor is known as the fourth basic passive circuit element characterized by its nonlinear relation between charge and magnetic flux and hysteresis loop in I-V plane. The first theoretical concept of memristor was postulated by L. Chua based on symmetric principle with rigorous mathematical proof [1]. The first experimental realization of memristor was confirmed by team of HP group in 2008 [2]. After the first realization of memristor, a large number of new applications areas have emerged in the last few years. The applications in the memory technology, neuromorphic hardware solution, soft computing, biomedical are only few of them [3-13].

The memristor is well suited for future resistive memory technology due to its high density of data storage, long data retention, low operating voltage, high endurance, fast read and write speed, lower programming current, fast switching speed and compatible with conventional CMOS process [14-15]. The memory property with resistance is a unique kind of feature, which leads to many application areas, particularly in circuit design. Recently, our research group developed nanostructured TiO_2 thin film memristor using hydrothermal process with low operation voltage (±0.68 V) [16]. In the point of view of circuit theory, Driscoll et al. reported memristive adaptive memory filter [17]. Talukdar et al. reported third-order autonomous linear time variant circuit based on memristor [18]. Pershin et al. reported memristor emulator and showed some of the applications of memristors in programmable analog circuit domain [19]. Kolka et al. reported frequency domain analysis of circuits with mem-elements and computed steady state analysis using harmonic balance method [20].

Considering the above facts and literature survey, memristor is a potential candidate for the next generation analog and digital circuits. In view of this, it is obligatory to investigate the performance and stability of memristor based circuits. The presents manuscript is also helpful for the undergraduate students to learn memristor dynamic and stability issues. In light of above facts, the present short communication discusses the state space analysis for memristor based series and parallel RLCM circuits. The stability analysis was carried out with the help of eigenvalues formulation method, pole-zero plot and transient response of system. In this investigation, we considered memristor as symmetric piecewise-linear driving-point (DP) nonlinear resistor, and at a high frequency, it behaves like a simple linear resistor [21]. The main contributions of the present paper are as follows:

- Simulated the nanostructured memristor using linear drift model reported in [2].
- We calculated the eigenvalues of both the systems and showed the systems are internally stable using pole-zero plot.
- The stability was also investigated using the system's responses to standard test signals (step and impulse).
- The BIBO stability was investigated using time and frequency domain analysis.
- We showed that the addition of memristor in circuit did not alter the performance of the system.

II. OVERVIEW OF MEMRISTOR

The memristor is a simple resistor with memory, and it is defined using the relationship between the charge and magnetic flux, as depicted in Equation (1). It is a fundamental and passive element due to the fact that there is no other combination of resistor, inductor and capacitor mimic with its pinched hysteresis loop in I-V plane. The fingerprint characteristics of memristor based on linear drift model are shown in Figure 1 (a and b). The simulation result clearly shows that Flux-Charge curve has nonlinear,

continuously differentiable, and monotonically increasing relation. This property made memristor a passive element. The slope of this curve represents the Memristance *M(q)*. The pinched hysteresis loop in the I-V plane is the fingerprint characteristics of memristor. This distinct property of memristor could not be realized in combination or alone by the other three passive circuit elements, hence memristor is a fundamental circuit element. The simulation realization of memristor was based on a linear dopant drift model with the state variable limited to the interval [0, D] and window function considered to be *f(x)=w(1-w)*. For the present simulation, the following parameters were kept constant: Input sinusoidal signal- V_M *sinwt*, where V_M = 1V, w = 2 Hz; Drift Velocity of oxygen vacancies = $\mu V = 10^{-14}$ $m^2V^{-1}s^{-1}$; D = 10 nm; w= 3 nm; R_{ON} = 75Ω; R_{OFF} = 16 KΩ; M-efficiency factor (R_{OFF}/R_{ON}) = 213.33.

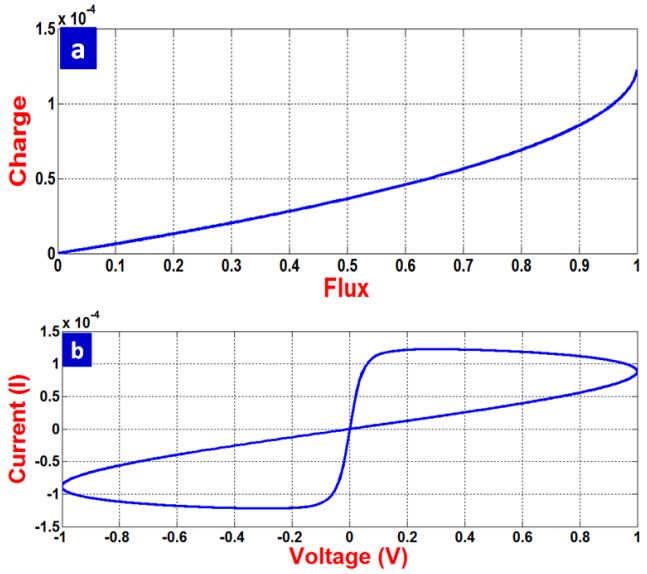

Figure 1: (A) Plot of Flux V/S Charge. (B) Plot of Current V/S Voltage.

Memristor does not store any charge itself but it is a totally dissipative circuit element [1]. L. Chua defined memristor based on state variable '*w*' and state variable either charge (current controlled memristor) or magnetic flux (voltage controlled memristor), defined in Equation (2) and (3) respectively [22].

$$\frac{d\varphi}{dq} = M \quad (1)$$

$$v = M(q)i \quad (2)$$

$$i = W(\varphi)v \quad (3)$$

The $M(q)$ and $W(\varphi)$ are known as memristance and memductance nonlinear functions where, *M (q)* is in the units of ohms and *W(φ)* is in Siemens [22]. The terminal quantities of memristor are given by Pershin et al. [15] and Kolka et al. [20, 23], based on their formulation,

$$V(t) = \frac{d\varphi(q)}{dt} = \frac{d\varphi(q)}{dq}\frac{dq}{dt} = R_M(q)\, i(t) \quad (4)$$

$$i(t) = \frac{dq(\varphi)}{dt} = \frac{dq(\varphi)}{d\varphi}\frac{d\varphi}{dt} = G_M(\varphi)\, V(t) \quad (5)$$

The $R_M(q)$ and $G_M(\varphi)$ are treated as memristance and memductance similar to Equation (2) and (3) respectively. For the sake of simplicity, we have concentrated our study only on current controlled memristor.

III. State Space Analysis

Figure 2 represents series connection of resistor (R), inductor (L), capacitor (C) and memristor (M) circuit. The circuit was excited by a sinusoidal signal *U(t)* and *i* is a total current flowing through the circuit. The V_L, V_R, V_C, and V_M are the voltage across inductor, resistor, capacitor and memristor respectively. The above circuit consists of two states variable V_C and I_L, and one output variable Y which are defined by Equation (6).

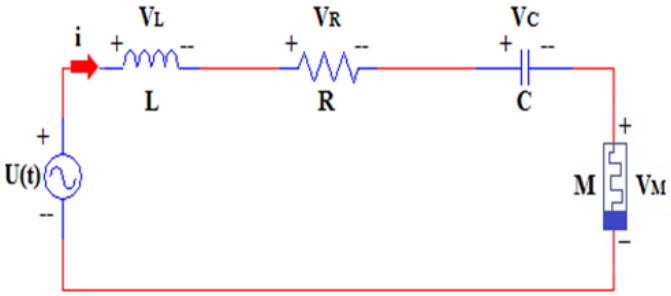

Figure 2: Series RLCM Circuit

$$\left.\begin{aligned} X_1 &= Vc \\ X_2 &= I_L \\ Y &= I_L \end{aligned}\right\} \quad (6)$$

Applying KVL to the above circuit we derive,

$$U(t) = V_L + V_R + V_C + V_M$$

$$U(t) = L\frac{dI_L}{dt} + R\, I_L + V_C + R_M(q)\, I_L$$

From the above equations, we get two relations regarding with the state variables,

$$\frac{dVc}{dt} = \frac{I_L}{C} \quad (7)$$

$$\frac{dI_L}{dt} = \frac{U}{L} - \frac{R}{L} I_L - \frac{1}{L} Vc - \frac{R_M(q)}{L} I_L \quad (8)$$

Rearranging the above Equation (7) and (8), we get:

$$\dot{X}_1 = \frac{X_2}{C} \quad (9)$$

$$\dot{X}_2 = \frac{U}{L} - \frac{R}{L} X_2 - \frac{1}{L} X_1 - \frac{R_M(q)}{L} X_2 \quad (10)$$

From Equation (9) and (10), we can write a state matrix in the form of $\dot{X} = Ax + B_U$ and $Y = Cx$, where $X = [X_1, X_2]^T$

$$\begin{bmatrix} \dot{X}_1 \\ \dot{X}_2 \end{bmatrix} = \begin{bmatrix} 0 & \frac{1}{C} \\ -\frac{1}{L} & -\left(\frac{R}{L} + \frac{R_M(q)}{L}\right) \end{bmatrix} \cdot \begin{bmatrix} X_1 \\ X_2 \end{bmatrix} + \begin{bmatrix} 0 \\ \frac{1}{L} \end{bmatrix} \cdot U \quad (11)$$

$$Y = [1 \quad 1] \cdot \begin{bmatrix} X_1 \\ X_2 \end{bmatrix} \quad (12)$$

Equation (11) and (12) represent the required state space representation of memristor based series RLCM circuit.

Figure 3 represents parallel connection of resistor (R), inductor (L), capacitor (C) and memristor (M) circuit. The circuit was excited by sinusoidal signal $Is(t)$ and I_R, I_L, I_C, and I_M are the current through resistor, inductor, capacitor, and memristor respectively. The above circuit consists of two states variable V_C and I_L and one output variable Y which are defined as follows:

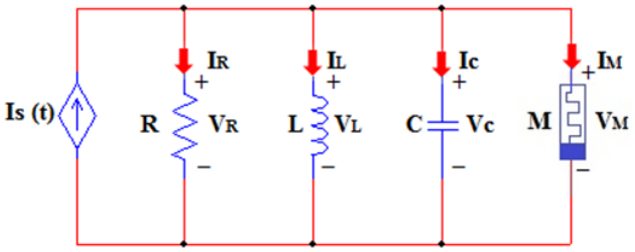

Figure 3: Parallel RLCM Circuit

$$\left.\begin{aligned} X_1 &= Vc \\ X_2 &= I_L \\ Y &= Vc \end{aligned}\right\} \tag{13}$$

Applying KCL to the above circuit we get:

$$I_S(t) = I_R + I_L + I_C + I_M$$

$$I_S(t) = \frac{Vc}{R} + I_L + C\frac{dVc}{dt} + \frac{Vc}{R_M(q)}$$

$$L\frac{dI_L}{dt} = Vc$$

From the above equations, we get two relations regarding with the state variables:

$$\frac{dVc}{dt} = -\frac{Vc}{RC} - \frac{I_L}{C} - \frac{Vc}{R_M(q)C} + \frac{Is}{C} \tag{14}$$

$$\frac{dI_L}{dt} = \frac{1}{L}Vc \tag{15}$$

Rearranging the above Equation (14) and (15), we get:

$$\dot{X}_1 = -\frac{X_1}{RC} - \frac{X_2}{C} - \frac{X_1}{R_M(q)C} + \frac{Is}{C} \tag{16}$$

$$\dot{X}_2 = \frac{1}{L}X_1 \tag{17}$$

From Equation (16) and (17), we can write a state matrix in the form of $\dot{X} = Ax + B_U$ and $Y = Cx$ where, $X = [X_1, X_2]^T$

$$\begin{bmatrix} \dot{X}_1 \\ \dot{X}_2 \end{bmatrix} = \begin{bmatrix} -\left(\frac{1}{RC} + \frac{1}{R_M(q)C}\right) & -\frac{1}{C} \\ \frac{1}{L} & 0 \end{bmatrix} \cdot \begin{bmatrix} X_1 \\ X_2 \end{bmatrix} + \begin{bmatrix} \frac{1}{C} \\ 0 \end{bmatrix} \cdot I_S \tag{18}$$

$$Y = \begin{bmatrix} 1 & 1 \end{bmatrix} \cdot \begin{bmatrix} X_1 \\ X_2 \end{bmatrix} \tag{19}$$

Equation (18) and (19) represent the required state space representation of memristor based the Parallel RLCM circuit.

The eigenvalues of memristor based series and parallel RLCM circuit are as follows,

$$\lambda_{1,2\,(\text{Series})} = -\left(\frac{R+R_M(q)}{2}\right) \pm \sqrt{\frac{C(R+R_M(q))^2 - 4}{LC}} \tag{20}$$

$$\lambda_{1,2\,(\text{Parallel})} = -\left(\frac{\left(\frac{1}{RC} + \frac{1}{R_M(q)C}\right) \pm \sqrt{\left(\frac{1}{RC} + \frac{1}{R_M(q)C}\right)^2 - 4\left(\frac{1}{LC}\right)}}{2}\right) \tag{21}$$

The equations (20 and 21) represent the eigenvalues of the memristor based series and parallel circuit respectively. It is clearly evident that eigenvalues have negative real part; and hence the above two systems are internally stable.

IV. Time and Frequency Domain Analysis of Series and Parallel RLCM Circuits

The pole-zero plot and system response to the standard test signal (step and impulse) are derived to define the stability of the system. The systems transient responses are depicted in Figure 4 (a-b) and pole-zero plots are shown in Figure 4 (c-d) respectively. The performance parameters of both the circuits are given in Table 1. For the present simulation, the following parameter were kept constant: R = 1 Ω, L = 0.1 H for series RLCM and RLC circuits and L = 1 H for parallel RLCM and RLC circuits, C = 1 F, and M = 1 Ω. It is clearly evident from Figure 4 (a-b) that the transient responses of systems posses BIBO stability. The result clearly indicates series RLCM circuit have a complex root with negative real parts and parallel RLCM circuit that have distinct root with negative real parts. The overall result shows the BIBO stability of the two systems.

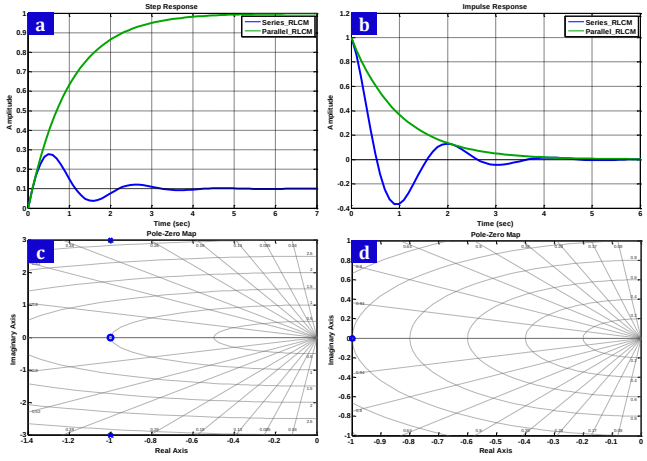

Figure 4: (a) Step Response of Series and parallel RLCM Circuit. (b): Impulse Response of Series and Parallel RLCM Circuit. (c): Pole-Zero map of Series RLCM Circuit. (d): Pole-Zero map of parallel RLCM Circuit.

For the comparison purpose, we calculated the state space matrix and eigenvalues of conventional series and parallel RLC circuits which are given in Equations (22) - (25) respectively.

$$\begin{bmatrix} \dot{X}_1 \\ \dot{X}_2 \end{bmatrix} = \begin{bmatrix} 0 & \frac{1}{C} \\ -\frac{1}{L} & -\frac{R}{L} \end{bmatrix} \cdot \begin{bmatrix} X_1 \\ X_2 \end{bmatrix} + \begin{bmatrix} 0 \\ \frac{1}{L} \end{bmatrix} \cdot U \tag{22}$$

$$\begin{bmatrix} \dot{X}_1 \\ \dot{X}_2 \end{bmatrix} = \begin{bmatrix} -\frac{1}{RC} & -\frac{1}{C} \\ \frac{1}{L} & 0 \end{bmatrix} \cdot \begin{bmatrix} X_1 \\ X_2 \end{bmatrix} + \begin{bmatrix} \frac{1}{C} \\ 0 \end{bmatrix} \cdot I_S \tag{23}$$

$$\lambda_{1,2\,(\text{Series})} = -\left(\frac{R}{2L}\right) \pm \sqrt{\frac{R^2}{4L^2} - \frac{1}{LC}} \tag{24}$$

$$\lambda_{1,2\,(\text{Parallel})} = -\left(\frac{1}{2RC}\right) \pm \sqrt{\frac{R^2}{4R^2C^2} - \frac{1}{LC}} \qquad (25)$$

The comparison of the memristor based series and parallel RLCM circuits with conventional RLC circuits are summarized in Table 1. It was observed that the memristor based circuits have lower peak amplitude, overshoot, peak time, and settling time than the conventional RLC circuits. Moreover, it was observed that the conventional series and parallel RLC circuits have a complex root with negative real parts and negative eigenvalues; hence, these systems are considered as stable systems. On the other hand, memristor based circuits also show the stability of BIBO. From the above results it can be concluded that the addition of memristor in circuit does not alter the performance of system.

Table 1
Performance Parameters of Series and Parallel RLCM and RLC Circuits

Performance Parameters		Series RLCM	Parallel RLCM	Series RLC	Parallel RLC
Peak Amplitude	Step Response	0.27	0.99	0.33	1.30
Overshoot (%)		177	0.00	240	30
Peak Time (s)		0.49	6.00	0.60	2.37
Rise Time (s)		0.08	2.20	0.08	0.939
Settling Time (s)		4.06	3.91	12	8.41
Final Value		0.10	1.00	0.10	1.00
Pole Location		α_1 = -1 + 3j and α_2 = -1-3j	-1	α_1 = -0.5+3j and α_2 = -0.5-3j	α_1 = -0.5+86j and α_2 = -0.5-86j
Zero Location		Z= -1	Z= -1	Z= -1	Z= -1
Peak Amplitude	Impulse Response	1.00	1.00	1.00	1.00
Settling Time (s)		5.00	3.91	9.45	9.63

The frequency domain response of memristor based series and parallel RLCM circuits are shown in Figs. 5(a-d). The Bode plot represents the magnitude and phase response of a system with respect to various frequencies. The maximum gain of series RLCM circuit is at 3 Hz and Parallel RLCM circuit at ~1 Hz. The gain is roll of -20dB/decade for both the circuits. This typical property can be utilized to design the memristor based on low pass and high pass filters [17, 24-25]. The Nyquist plot for memristor based series and parallel RLCM circuits are shown in Figure 5(b). The Nyquist plot shows the frequency and amplitude response of a system in a single plot. In other words, it is a polar plot in the frequency domain of a linear system. The series RLCM circuit shows the two poles at α_1 = -1 + 3j and α_2 = -1 - 3j; hence, at high frequencies, the asymptote is at -180°. The two poles and one zero property of series RLCM circuit are similar to second order system characteristics. The parallel RLCM circuit consists of only one zero with the absence of pole, which results in a perfect circle, like the characteristics with asymptote at -90°. From the Nyquist plot, it is clearly seen that the series and parallel RLCM systems possess the BIBO stability.

Figure 5(c) represents the Nichols plot of series and parallel RLCM circuit and 5(d) represents the Hankel Singular value plot of the system. The Nichols plot is a magnitude and phase plot with varying frequencies similar to Bode and Nyquist plot. The Nichols plot is a special case in frequency domain, in which the system response consists of an open loop response with transient response of system [26]. The Hankel Singular value plot represents the stable modes of a system. From both plots, it is clearly seen that the system possessed BIBO stability.

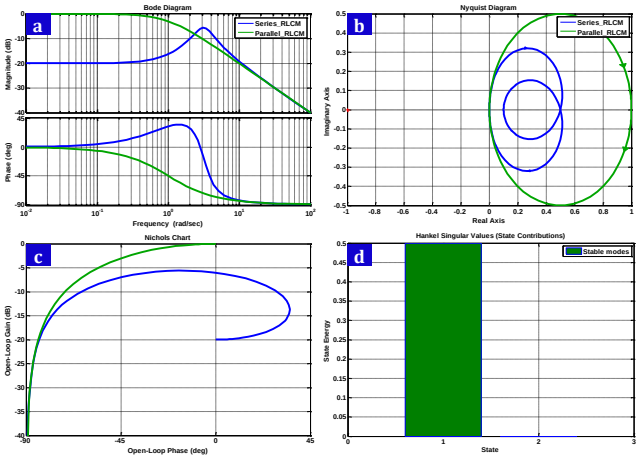

Figure 5: (a) The Bode Plot of Memristor based Series and Parallel RLCM Circuits. (b) The Nyquist Plot of Memristor based Series and Parallel RLCM Circuits. (c) The Nichols Plot of Memristor based Series and Parallel RLCM Circuits. (d) Hankel Singular value plot of the system.

V. CONCLUSION

The present paper deals with the state space analysis of memristor based series and parallel circuits. The state space analysis with eigenvalues methodology was adopted to investigate stability. The systems have negative real part of eigenvalues, hence the above two systems are internally stable. It simply means that the pole of systems is located at left hand side of '*S*' plane. The responses of the system to the standard test signal (step and impulse) also show the stability of systems. The results of the time and frequency domain of both systems also suggest BIBO stability. The comparison of the memristor based series and parallel RLCM circuits with conventional RLC circuits also suggest that the addition of memristor in circuit does not alter the performance of the system. As a part of the current research, time and frequency domain simulation of series and parallel RLCM circuits were demonstrated. However, the scope of the future research is to develop series and parallel RLCM circuits using off-the-shelf circuit components (*R*, *L*, and *C*) and hydrothermally synthesized micro memristor. We would like to compare the simulation results and experimental results in the next stage of research.

ACKNOWLEDGMENT

Authors are very much thankful to Prof. P. S. Patil for providing computational facilities and Dr. P. J. Patil for fruitful discussions on the state space representation.

REFERENCES

[1] L. Chua, "Memristor-The missing circuit element," *IEEE Trans. Circuit Theory*, vol. 18, no. 5, pp. 507–519, 1971.

[2] D. B. Strukov, G. S. Snider, D. R. Stewart, and R. S. Williams, "The missing memristor found," *Nature*, vol. 453, no. 7191, pp. 80–83, May 2008.

[3] T. D. Dongale, N. D. Desai, K. V. Khot, N. B. MullaniP. S. Pawar, R. S. Tikke, V. B. Patil, P. P. Waifalkar, P. B. Patil, R. K. Kamat, P. S. Patil, "Effect of surfactants on the data directionality and learning behaviour of Al/TiO_2/FTO thin film memristor-based electronic synapse," *J. Solid State Electr.*, pp.1-5, 2016, DOI: 10.1007/s10008-016-3459-1.

[4] T. D. Dongale, K. P. Patil, S. R. Vanjare, A. R. Chavan, P. K. Gaikwad, and R. K. Kamat, "Modelling of nanostructured memristor device characteristics using artificial neural network (ANN)," *J. Comput. Sci.*, vol. 11, pp. 82–90, Nov. 2015.

[5] T. D. Dongale, S. V. Mohite, A. A. Bagade, P. K. Gaikwad, P. S. Patil, R. K. Kamat, K. Y. Rajpure, "Development of Ag/WO_3/ITO thin film memristor using spray pyrolysis method," *Electron. Mater. Lett.*, vol. 11, no. 6, pp. 944–948, Oct. 2015.

[6] T. D. Dongale, K. P. Patil, P. K. Gaikwad, and R. K. Kamat, "Investigating conduction mechanism and frequency dependency of nanostructured memristor device," *Mater. Sci. Semicond. Process.*, vol. 38, pp. 228–233, Oct. 2015.

[7] T. D. Dongale, K. V. Khot, S. S. Mali, P. S. Patil, P. K. Gaikwad, R. K. Kamat, P. N. Bhosale, "Development of Ag/ZnO/FTO thin film memristor using aqueous chemical route," *Mater. Sci. Semicond. Process.*, vol. 40, pp. 523–526, Dec. 2015.

[8] T. D. Dongale, K. P. Patil, S. B. Mullani, K. V. More, S. D. Delekar, P. S. Patil, P. K. Gaikwad, R. K. Kamat, "Investigation of process parameter variation in the memristor based resistive random access memory (RRAM): Effect of device size variations," *Mater. Sci. Semicond. Process.*, vol. 35, pp. 174–180, Jul. 2015.

[9] S. S. Shinde and T. D. Dongle, "Modelling of nanostructured TiO2-based memristors," *J. Semicond.*, vol. 36, no. 3, p. 034001, Mar. 2015.

[10] T. D. Dongale, P. J. Patil, K. P. Patil, S. B. Mullani, K. V. More, S. D. Delekar, P. K. Gaikwad, R. K. Kamat, "Piecewise Linear and Nonlinear Window Functions for Modelling of Nanostructured Memristor Device," *J. Nano. Electron. Phy.*, vol. 7, no. 3, pp. 03012-1-03012-4, 2015.

[11] T. D. Dongale, P. S. Pawar, R. S. Tikke, N. B. Mullani, V. B. Patil, A. M. Teli, K. V. Khot, S. V. Mohite, A. A. Bagade, V. S. Kumbhar, K. Y. Rajpure, P. N. Bhosale, R. K. Kamat, P. S. Patil, "Mimicking the synaptic weights and human forgetting curve using hydrothermally grown nanostructured CuO memristor device," *J. Nanosci. Nanotechnol.*, vol. 17, pp.1–8, 2017.

[12] T. D. Dongale, K. V. Khot, S. V. Mohite, S. S. Khandagale, S. S. Shinde, V. L. Patil, S. A. Vanalkar, A. V. Moholkar, K. Y. Rajpure, P. N. Bhosale, P. S. Patil, P. K. Gaikwad, R. K. Kamat, "Investigating the Temperature Effects on ZnO, TiO_2, WO_3 and HfO_2 Based Resistive Random Access Memory (RRAM) Devices," *J. Nano. Electron. Phy.*, vol. 8, no. 4, pp. 04030-1-04030-4, 2016.

[13] T. D. Dongale, P. J. Patil, N. K. Desai, P. P. Chougule, S. M. Kumbhar, P. P. Waifalkar, P. B. Patil, R. S. Vhatkar, M. V., Takale, P. K. Gaikwad, and R. K. Kamat, "TiO_2 based nanostructured memristor for RRAM and neuromorphic applications: A simulation approach," *Nano Convergence*, vol. 3, no. 1, pp. 1-7, July 2016.

[14] L. M. Kukreja, A. K. Das, and P. Misra, "Studies on nonvolatile resistance memory switching in ZnO thin films," *Bull. Mater. Sci.*, vol. 32, no. 3, pp. 247–252, Jun. 2009.

[15] Y. V. Pershin and M. Di Ventra, "Memory effects in complex materials and nanoscale systems," *Adv. Phys.*, vol. 60, no. 2, pp. 145–227, Apr. 2011.

[16] T. D. Dongale, S. S. Shinde, R. K. Kamat, and K. Y. Rajpure, "Nanostructured TiO_2 thin film memristor using hydrothermal process," *J. Alloys Compd.*, vol. 593, pp. 267–270, Apr. 2014.

[17] T. Driscoll, J. Quinn, S. Klein, H. T. Kim, B. J. Kim, Y. V. Pershin, M. D. Ventra & D. N. Basov, "Memristive adaptive filters," *Appl. Phys. Lett.*, vol. 97, no. 9, p. 093502, 2010.

[18] A. Talukdar, A. G. Radwan, and K. N. Salama, "A memristor-based third-order oscillator: Beyond oscillation," *Appl Nanosci.*, vol. 1, no. 3, pp. 143–145, Aug. 2011.

[19] Y. V. Pershin and M. Di Ventra, "Practical approach to programmable analog circuits with Memristors," *IEEE Trans. Circuits Syst. I, Reg. Papers.*, vol. 57, no. 8, pp. 1857–1864, Aug. 2010.

[20] Z. Kolka, D. Biolek, and V. Biolkova, "Frequency-domain steady-state analysis of circuits with mem-elements," *Analog Integr. Circuits Signal Process.*, vol. 74, no. 1, pp. 79–89, Aug. 2012.

[21] Y. N. Joglekar and S. J. Wolf, "The elusive memristor: Properties of basic electrical circuits," *Eur. J. Phys.*, vol. 30, no. 4, pp. 661–675, May 2009.

[22] M. Itoh and L. O. Chua, "Duality Of Memristor Circuits," *Int J Bifurcat Chaos.*, vol. 23, no. 01, p. 1330001, Jan. 2013.

[23] V. Biolkova, Z. Kolka, D. Biolek, & Z. Biolek, "Memristor modeling based on its constitutive relation," In *Proc. Eur. Conf. Circuits Tech. & Devices*, 2010, pp. 261–264.

[24] H. H. C. Iu, D. S. Yu, A. L. Fitch, V. Sreeram, and H. Chen, "Controlling chaos in a Memristor based circuit using a twin-t notch filter," *IEEE Trans. Circuits Syst. I, Reg. Papers.*, vol. 58, no. 6, pp. 1337–1344, Jun. 2011.

[25] S. Jameel, C. Korasli, and A. Nacaroglu, "Realization of biquadratic filter by using memristor," In *IEEE Int. Conf. Tech. Adv Elect., Electro. & Comp. Eng. (TAEECE)*, 2013, pp. 52-56.

[26] N. Cohen, Y. Chait, O. Yaniv, and C. Borghesani, "Stability analysis using Nichols charts," *Int. J. Robust. Nonlin.*, vol. 4, no. 1, pp. 3–20, 1994.